Journal of Applied Mathematics and Mechanics

ZAMM

Zeitschrift für Angewandte Mathematik und Mechanik
Founded by Richard von Mises in 1921

Elastic fields due to a rectangular inclusion with uniform antiplane eigenstrains in a bimaterial consisting of two orthotropic quarter planes

X. Wang and **E. Pan**

Department of Civil Engineering and Department of Applied Mathematics, University of Akron, Akron, OH 44325-3905, USA

Received 4 April 2008, revised and accepted 1 July 2008
Published online 26 September 2008

Key words Rectangular inclusion, Green's function, orthotropic, quarter plane.

The Green's function method is employed to derive closed-form solutions for displacement, strains, and stresses due to a rectangular inclusion with uniform antiplane eigenstrains in an orthotropic quarter plane and in a bimaterial composed of two orthotropic quarter planes bonded together. It is observed that both the strains and stresses exhibit logarithmic singularity near the four vertices of the rectangular inclusion. Numerical results are also presented to show the distribution of the eigenstrain-induced displacement and stress fields in the quarter planes.

Z. Angew. Math. Mech. **88**, No. 10, 817 – 827 (2008) / **DOI** 10.1002/zamm.200800064

www.zamm-journal.org

WILEY-VCH

ZAMM · Z. Angew. Math. Mech. **88**, No. 10, 817 – 827 (2008) / **DOI** 10.1002/zamm.200800064

Elastic fields due to a rectangular inclusion with uniform antiplane eigenstrains in a bimaterial consisting of two orthotropic quarter planes

X. Wang* **and E. Pan****

Department of Civil Engineering and Department of Applied Mathematics, University of Akron, Akron, OH 44325-3905, USA

Received 4 April 2008, revised and accepted 1 July 2008
Published online 26 September 2008

Key words Rectangular inclusion, Green's function, orthotropic, quarter plane.

The Green's function method is employed to derive closed-form solutions for displacement, strains, and stresses due to a rectangular inclusion with uniform antiplane eigenstrains in an orthotropic quarter plane and in a bimaterial composed of two orthotropic quarter planes bonded together. It is observed that both the strains and stresses exhibit logarithmic singularity near the four vertices of the rectangular inclusion. Numerical results are also presented to show the distribution of the eigenstrain-induced displacement and stress fields in the quarter planes.

1 Introduction

Polygonal or facetted Eshelby's inclusions with uniform eigenstrains will induce singular stresses and strains near some sharp corners and edges of these inclusions [1–4]. Here the inclusion and the surrounding matrix possess the same elastic constants. The solutions of facetted inclusions in an infinite medium have been extended to the case of these kinds of inclusions in a half-space. Chiu [5] first discussed a parallelepipedic inclusion in a half-space. The elastic fields were obtained in terms of Legendre polynomials [5]. Hu [6] obtained an analytical solution in terms of elementary functions for the stress fields outside a thermal parallelepipedic inclusion embedded in a half-space. Glas [7] derived closed-form expressions in terms of elementary functions for the displacements, strains, stresses, and strain energy induced by a thermal parallelepipedic inclusion in a half-space. Hu [6] and Glas [7] also obtained the elastic field due to a rectangular inclusion of infinite length oriented parallel to the free surface. Recently the anisotropic and piezoelectric properties of the facetted inclusions and the surrounding matrix were also taken into consideration to simulate and predict the behavior of strained quantum wire semiconductor structures [4, 8, 9]. We remark that all the listed results are constrained to the case where the parallelepipedic inclusion interacts with only one boundary or interface. The polygonal inclusion problem in a domain bounded by more than one boundary has not been solved so far.

By virtue of the image method, Ting [10] recently derived the Green's functions due to an antiplane force and a screw dislocation in a quarter plane and a bimaterial consisting of two quarter planes that are bonded together. His result shows that the number of images is *finite* for an orthotropic quarter plane and for two bonded orthotropic quarter planes under antiplane deformations. This property of the Green's functions for a quarter plane makes it possible to investigate the elastic field induced by a rectangular inclusion of uniform antiplane eigenstrains which is embedded in an orthotropic quarter plane and in two bonded orthotropic quarter planes.

In this paper, Ting's Green's function solutions [10] for an orthotropic quarter plane and a bimaterial consisting of two orthotropic quarter planes are utilized to derive the elastic fields (i.e., the displacement, strains, and stresses) induced by a rectangular inclusion with uniform antiplane eigenstrains embedded in an orthotropic quarter plane and in a bimaterial composed of two orthotropic quarter planes bonded together. Since the expressions for the displacement, strains, and stresses involve only elementary functions, the main features of the induced elastic fields, such as the singularity, discontinuity, etc, are clearly shown from these expressions, as further demonstrated also by typical numerical examples.

* Corresponding author, e-mail: xuwang@uakron.edu
** E-mail: pan2@uakron.edu

2 Basic formulations

In a fixed Cartesian coordinate system, the stress-strain relation for an antiplane deformation of an orthotropic material with eigenstrains is

$$\sigma_{31} = C_{55}(u_{,1} - 2\varepsilon^*_{31}),\ \sigma_{32} = C_{44}(u_{,2} - 2\varepsilon^*_{32}), \tag{1}$$

where the subscript "$,i$" denotes the derivative with respect to the i-th coordinate x_i $(i = 1, 2)$, $u = u_3$ the total out-of-plane displacement, σ_{32} and σ_{31} the stress components, C_{44} and C_{55} the elastic constants, and ε^*_{31} and ε^*_{32} are the uniform antiplane eigenstrains within the rectangular inclusion Ω. These eigenstrains are zero outside the inclusion domain. The equation of equilibrium is

$$\sigma_{31,1} + \sigma_{32,2} = 0 \tag{2}$$

or equivalently

$$C_{55}u_{,11} + C_{44}u_{,22} = 2C_{55}\varepsilon^*_{31,1} + 2C_{44}\varepsilon^*_{32,2}. \tag{3}$$

According to Mura [2], the displacement field can be expressed in terms of integration along the boundary of the inclusion, as

$$u = 2C_{55}\varepsilon^*_{31}\int_{\partial\Omega} G(\mathbf{x}, \mathbf{x}')n_1 \mathrm{d}l + 2C_{44}\varepsilon^*_{32}\int_{\partial\Omega} G(\mathbf{x}, \mathbf{x}')n_2 \mathrm{d}l, \tag{4}$$

where $\partial\Omega$ is the boundary of the inclusion Ω, and the integration is with respect to the source point $\mathbf{x}'$ of the Green's function $G(\mathbf{x}, \mathbf{x}')$. The above expression indicates that once the Green's function is known, the induced displacement can be found by simply carrying out the line integral in Eq. (4). Making use of Ting's recent results [10], we present the exact closed-form solution due to a rectangular inclusion for the displacement, and strain and stress fields in the next sections.

3 A rectangular inclusion in a quarter plane

Let the material occupy the quarter plane $x_1 \geq 0$ and $x_2 \geq 0$, as shown in Fig. 1. In addition the rectangular inclusion occupies the region $\Omega:\ a_1 \leq x_1 \leq a_2$ and $b_1 \leq x_2 \leq b_2$ $(a_1, a_2 \geq 0,\ b_1, b_2 \geq 0)$. Recently Ting [10] has obtained explicit expressions of the Green's function for an orthotropic quarter plane. In his solutions, four boundary conditions on the surfaces $x_1 = 0$ and $x_2 = 0$ are considered: 1) Free-free ($x_1 = 0$ and $x_2 = 0$ are traction free); 2) Fixed-fixed ($x_1 = 0$ and $x_2 = 0$ are fixed); 3) Free-fixed ($x_1 = 0$ is traction free and $x_2 = 0$ is fixed); 4) Fixed-free ($x_1 = 0$ is fixed and $x_2 = 0$ is traction free). It is found that the line integrals in Eq. (4) can be explicitly performed by employing the Green's functions for a quarter plane [10]. In the following we present the total displacement, total strains, and elastic stresses for the four boundary conditions.

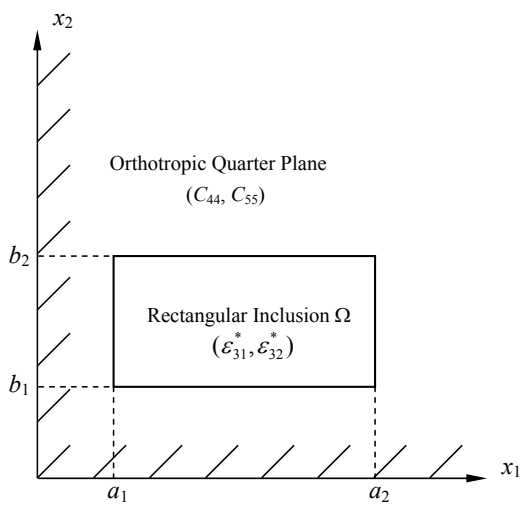

Fig. 1 A rectangular inclusion with uniform antiplane eigenstrains ε^*_{31} and ε^*_{32} embedded in an orthotropic quarter plane.

3.1 Free-free quarter plane

The explicit expression of the total displacement is given by

$$\begin{aligned} u =& \frac{\varepsilon_{31}^*}{\pi}\left[f(a_1,a_2,b_1,b_2) - f(a_1,a_2,-b_1,-b_2) - f(-a_1,-a_2,-b_1,-b_2) + f(-a_1,-a_2,b_1,b_2)\right] \\ &+ \frac{\varepsilon_{32}^*}{\pi\gamma}\left[g(a_1,a_2,b_1,b_2) + g(a_1,a_2,-b_1,-b_2) - g(-a_1,-a_2,-b_1,-b_2) - g(-a_1,-a_2,b_1,b_2)\right], \end{aligned} \tag{5}$$

where $\gamma = \sqrt{C_{55}/C_{44}}$ and

$$\begin{aligned} f(a_1,a_2,b_1,b_2) &= \sum_i\sum_j (-1)^{i+j}\left(\bar{y}_j \ln\sqrt{\bar{x}_i^2+\bar{y}_j^2} + \bar{x}_i \tan^{-1}\frac{\bar{y}_j}{\bar{x}_i}\right), \\ g(a_1,a_2,b_1,b_2) &= \sum_i\sum_j (-1)^{i+j}\left(\bar{x}_i \ln\sqrt{\bar{x}_i^2+\bar{y}_j^2} + \bar{y}_j \tan^{-1}\frac{\bar{x}_i}{\bar{y}_j}\right), \end{aligned} \tag{6}$$

with $i, j = 1, 2$, and

$$\bar{x}_1 = x_1 - a_1,\ \bar{x}_2 = x_1 - a_2,\ \bar{y}_1 = \gamma(x_2 - b_1),\ \bar{y}_2 = \gamma(x_2 - b_2). \tag{7}$$

If we define the following four rectangular regions A, B, C, D as

$$\begin{aligned} A:&\ a_1 \le x_1 \le a_2,\ b_1 \le x_2 \le b_2 \\ B:&\ a_1 \le x_1 \le a_2,\ -b_2 \le x_2 \le -b_1, \\ C:&\ -a_2 \le x_1 \le -a_1,\ -b_2 \le x_2 \le -b_1, \\ D:&\ -a_2 \le x_1 \le -a_1,\ b_1 \le x_2 \le b_2, \end{aligned} \tag{8}$$

then Eq. (5) indicates that the induced total displacement can be considered as the superposition of four rectangular inclusions (region A with eigenstrains ε_{31}^* and ε_{32}^*, image region B with eigenstrains ε_{31}^* and $-\varepsilon_{32}^*$, image region C with eigenstrains $-\varepsilon_{31}^*$ and $-\varepsilon_{32}^*$, and image region D with eigenstrains $-\varepsilon_{31}^*$ and ε_{32}^*) in an infinite orthotropic plane.

The explicit expressions of the total strains are obtained by taking the derivative of the induced displacement, which are given by

$$\begin{aligned} \gamma_{31} =& \frac{\varepsilon_{31}^*}{\pi}\left[f_1(a_1,a_2,b_1,b_2) - f_1(a_1,a_2,-b_1,-b_2) - f_1(-a_1,-a_2,-b_1,-b_2) + f_1(-a_1,-a_2,b_1,b_2)\right] \\ &+ \frac{\varepsilon_{32}^*}{\pi\gamma}\left[g_1(a_1,a_2,b_1,b_2) + g_1(a_1,a_2,-b_1,-b_2) - g_1(-a_1,-a_2,-b_1,-b_2) - g_1(-a_1,-a_2,b_1,b_2)\right], \end{aligned} \tag{9}$$

$$\begin{aligned} \gamma_{32} =& \frac{\varepsilon_{31}^*}{\pi}\left[f_2(a_1,a_2,b_1,b_2) - f_2(a_1,a_2,-b_1,-b_2) - f_2(-a_1,-a_2,-b_1,-b_2) + f_2(-a_1,-a_2,b_1,b_2)\right] \\ &+ \frac{\varepsilon_{32}^*}{\pi\gamma}\left[g_2(a_1,a_2,b_1,b_2) + g_2(a_1,a_2,-b_1,-b_2) - g_2(-a_1,-a_2,-b_1,-b_2) - g_2(-a_1,-a_2,b_1,b_2)\right], \end{aligned} \tag{10}$$

where $\gamma_{31} = u_{,1},\ \gamma_{32} = u_{,2}$ and

$$\begin{aligned} f_1(a_1,a_2,b_1,b_2) &= \sum_i\sum_j (-1)^{i+j}\tan^{-1}\frac{\bar{y}_j}{\bar{x}_i},\ f_2(a_1,a_2,b_1,b_2) = \gamma\sum_i\sum_j (-1)^{i+j}\ln\sqrt{\bar{x}_i^2+\bar{y}_j^2}, \\ g_1(a_1,a_2,b_1,b_2) &= \sum_i\sum_j (-1)^{i+j}\ln\sqrt{\bar{x}_i^2+\bar{y}_j^2},\ g_2(a_1,a_2,b_1,b_2) = \gamma\sum_i\sum_j (-1)^{i+j}\tan^{-1}\frac{\bar{x}_i}{\bar{y}_j}. \end{aligned} \tag{11}$$

Consequently, the stress components can be obtained from Eq. (1) with the strains given in Eqs. (9) and (10). Based on the solutions of the strain and stress, one can immediately observe the following interesting features: 1) on the interfaces $x_1 = a_1$ and $x_1 = a_2$, the strain and stress components γ_{32} and σ_{31} are continuous, whilst the other strain and stress components γ_{31} and σ_{32} are discontinuous; additionally $\gamma_{31}^{\text{inclusion}} - \gamma_{31}^{\text{matrix}} = 2\varepsilon_{31}^*$ and $\sigma_{32}^{\text{inclusion}} - \sigma_{32}^{\text{matrix}} = -2C_{44}\varepsilon_{32}^*$; 2) on

the interfaces $x_2 = b_1$ and $x_2 = b_2$, the strain and stress components γ_{31} and σ_{32} are continuous, whilst the other strain and stress components γ_{32} and σ_{31} are discontinuous; additionally $\gamma_{32}^{\text{inclusion}} - \gamma_{32}^{\text{matrix}} = 2\varepsilon_{32}^*$ and $\sigma_{31}^{\text{inclusion}} - \sigma_{31}^{\text{matrix}} = -2C_{55}\varepsilon_{31}^*$; 3) γ_{31} and σ_{31} exhibit logarithmic singularities near the four corners of the rectangular inclusion when $\varepsilon_{32}^* \neq 0$, whilst γ_{32} and σ_{32} exhibit logarithmic singularities near the four corners of the rectangular inclusion when $\varepsilon_{31}^* \neq 0$; 4) the second-order antiplane Eshelby's tensor **S**, which is defined as $\gamma_{3i} = 2S_{ij}\varepsilon_{3j}^*$, is non-uniform inside the rectangular inclusion. It shall be mentioned that these properties along the inclusion-matrix interfaces and at the corners are independent of the type of the boundary conditions along the two boundaries of the quarter plane.

3.2 Fixed-fixed quarter plane

The explicit expression of the total displacement is given by

$$\begin{aligned} u =& \frac{\varepsilon_{31}^*}{\pi}\left[f(a_1,a_2,b_1,b_2) + f(a_1,a_2,-b_1,-b_2) - f(-a_1,-a_2,-b_1,-b_2) - f(-a_1,-a_2,b_1,b_2)\right] \\ &+ \frac{\varepsilon_{32}^*}{\pi\gamma}\left[g(a_1,a_2,b_1,b_2) - g(a_1,a_2,-b_1,-b_2) - g(-a_1,-a_2,-b_1,-b_2) + g(-a_1,-a_2,b_1,b_2)\right]. \end{aligned} \tag{12}$$

The above expression indicates that the induced total displacement can be considered as the superposition of four rectangular inclusions (region A with eigenstrains ε_{31}^* and ε_{32}^*, image region B with eigenstrains $-\varepsilon_{31}^*$ and ε_{32}^*, image region C with eigenstrains $-\varepsilon_{31}^*$ and $-\varepsilon_{32}^*$, and image region D with eigenstrains ε_{31}^* and $-\varepsilon_{32}^*$) in an infinite plane.

Similarly, the explicit expressions of the total strains are given by

$$\begin{aligned} \gamma_{31} =& \frac{\varepsilon_{31}^*}{\pi}\left[f_1(a_1,a_2,b_1,b_2) + f_1(a_1,a_2,-b_1,-b_2) - f_1(-a_1,-a_2,-b_1,-b_2) - f_1(-a_1,-a_2,b_1,b_2)\right] \\ &+ \frac{\varepsilon_{32}^*}{\pi\gamma}\left[g_1(a_1,a_2,b_1,b_2) - g_1(a_1,a_2,-b_1,-b_2) - g_1(-a_1,-a_2,-b_1,-b_2) + g_1(-a_1,-a_2,b_1,b_2)\right], \end{aligned} \tag{13}$$

$$\begin{aligned} \gamma_{32} =& \frac{\varepsilon_{31}^*}{\pi}\left[f_2(a_1,a_2,b_1,b_2) + f_2(a_1,a_2,-b_1,-b_2) - f_2(-a_1,-a_2,-b_1,-b_2) - f_2(-a_1,-a_2,b_1,b_2)\right] \\ &+ \frac{\varepsilon_{32}^*}{\pi\gamma}\left[g_2(a_1,a_2,b_1,b_2) - g_2(a_1,a_2,-b_1,-b_2) - g_2(-a_1,-a_2,-b_1,-b_2) + g_2(-a_1,-a_2,b_1,b_2)\right]. \end{aligned} \tag{14}$$

3.3 Free-fixed quarter plane

The explicit expression of the total displacement is given by

$$\begin{aligned} u =& \frac{\varepsilon_{31}^*}{\pi}\left[f(a_1,a_2,b_1,b_2) + f(a_1,a_2,-b_1,-b_2) + f(-a_1,-a_2,-b_1,-b_2) + f(-a_1,-a_2,b_1,b_2)\right] \\ &+ \frac{\varepsilon_{32}^*}{\pi\gamma}\left[g(a_1,a_2,b_1,b_2) - g(a_1,a_2,-b_1,-b_2) + g(-a_1,-a_2,-b_1,-b_2) - g(-a_1,-a_2,b_1,b_2)\right]. \end{aligned} \tag{15}$$

The above expression indicates that the induced total displacement can be considered as the superposition of four rectangular inclusions (region A with eigenstrains ε_{31}^* and ε_{32}^*, image region B with eigenstrains $-\varepsilon_{31}^*$ and ε_{32}^*, image region C with eigenstrains ε_{31}^* and ε_{32}^*, and image region D with eigenstrains $-\varepsilon_{31}^*$ and ε_{32}^*) in an infinite plane.

The explicit expressions of the total strains are given by

$$\begin{aligned} \gamma_{31} =& \frac{\varepsilon_{31}^*}{\pi}\left[f_1(a_1,a_2,b_1,b_2) + f_1(a_1,a_2,-b_1,-b_2) + f_1(-a_1,-a_2,-b_1,-b_2) + f_1(-a_1,-a_2,b_1,b_2)\right] \\ &+ \frac{\varepsilon_{32}^*}{\pi\gamma}\left[g_1(a_1,a_2,b_1,b_2) - g_1(a_1,a_2,-b_1,-b_2) + g_1(-a_1,-a_2,-b_1,-b_2) - g_1(-a_1,-a_2,b_1,b_2)\right], \end{aligned} \tag{16}$$

$$\begin{aligned} \gamma_{32} =& \frac{\varepsilon_{31}^*}{\pi}\left[f_2(a_1,a_2,b_1,b_2) + f_2(a_1,a_2,-b_1,-b_2) + f_2(-a_1,-a_2,-b_1,-b_2) + f_2(-a_1,-a_2,b_1,b_2)\right] \\ &+ \frac{\varepsilon_{32}^*}{\pi\gamma}\left[g_2(a_1,a_2,b_1,b_2) - g_2(a_1,a_2,-b_1,-b_2) + g_2(-a_1,-a_2,-b_1,-b_2) - g_2(-a_1,-a_2,b_1,b_2)\right]. \end{aligned} \tag{17}$$

3.4 Fixed-free quarter plane

The explicit expression of the total displacement is given by

$$\begin{aligned} u =& \frac{\varepsilon_{31}^*}{\pi}\left[f(a_1,a_2,b_1,b_2) - f(a_1,a_2,-b_1,-b_2) + f(-a_1,-a_2,-b_1,-b_2) - f(-a_1,-a_2,b_1,b_2)\right] \\ &+ \frac{\varepsilon_{32}^*}{\pi\gamma}\left[g(a_1,a_2,b_1,b_2) + g(a_1,a_2,-b_1,-b_2) + g(-a_1,-a_2,-b_1,-b_2) + g(-a_1,-a_2,b_1,b_2)\right]. \end{aligned} \tag{18}$$

The above expression indicates that the induced total displacement can be considered as the superposition of four rectangular inclusions (region A with eigenstrains ε_{31}^* and ε_{32}^*, region B with eigenstrains ε_{31}^* and $-\varepsilon_{32}^*$, region C with eigenstrains ε_{31}^* and ε_{32}^*, and region D with eigenstrains ε_{31}^* and $-\varepsilon_{32}^*$) in an infinite plane.

The explicit expressions of the total strains are given by

$$\begin{aligned} \gamma_{31} =& \frac{\varepsilon_{31}^*}{\pi}\left[f_1(a_1,a_2,b_1,b_2) - f_1(a_1,a_2,-b_1,-b_2) + f_1(-a_1,-a_2,-b_1,-b_2) - f_1(-a_1,-a_2,b_1,b_2)\right] \\ &+ \frac{\varepsilon_{32}^*}{\pi\gamma}\left[g_1(a_1,a_2,b_1,b_2) + g_1(a_1,a_2,-b_1,-b_2) + g_1(-a_1,-a_2,-b_1,-b_2) + g_1(-a_1,-a_2,b_1,b_2)\right], \end{aligned} \tag{19}$$

$$\begin{aligned} \gamma_{32} =& \frac{\varepsilon_{31}^*}{\pi}\left[f_2(a_1,a_2,b_1,b_2) - f_2(a_1,a_2,-b_1,-b_2) + f_2(-a_1,-a_2,-b_1,-b_2) - f_2(-a_1,-a_2,b_1,b_2)\right] \\ &+ \frac{\varepsilon_{32}^*}{\pi\gamma}\left[g_2(a_1,a_2,b_1,b_2) + g_2(a_1,a_2,-b_1,-b_2) + g_2(-a_1,-a_2,-b_1,-b_2) + g_2(-a_1,-a_2,b_1,b_2)\right]. \end{aligned} \tag{20}$$

4 A rectangular inclusion in a bimaterial

In this section we add a second orthotropic material in the quarter plane $x_1 \geq 0$ and $x_2 \leq 0$, as shown in Fig. 2. In addition, we assume that the upper quarter plane and the lower quarter plane are well bonded along the interface $x_2 = 0,\ x_1 \geq 0$ (displacement and traction are continuous). Ting [10] has also presented explicit expressions of the Green's function for this bimaterial composed of two orthotropic quarter planes. Employing his Green's functions for the bimaterial, we can arrive at the solutions for two cases: 1) the boundary $x_1 = 0$ is traction free; 2) the boundary $x_1 = 0$ is fixed. In what follows we add a prime ' to the quantities associated with the lower quarter plane.

When the boundary $x_1 = 0$ is traction free, the total displacement in the upper quarter plane can be expressed as

$$\begin{aligned} u =& \frac{\varepsilon_{31}^*}{\pi}\left[f(a_1,a_2,b_1,b_2) - \xi f(a_1,a_2,-b_1,-b_2) - \xi f(-a_1,-a_2,-b_1,-b_2) + f(-a_1,-a_2,b_1,b_2)\right] \\ &+ \frac{\varepsilon_{32}^*}{\pi\gamma}\left[g(a_1,a_2,b_1,b_2) + \xi g(a_1,a_2,-b_1,-b_2) - \xi g(-a_1,-a_2,-b_1,-b_2) - g(-a_1,-a_2,b_1,b_2)\right], \end{aligned} \tag{21}$$

and the total displacement in the lower quarter plane is

$$u' = \frac{\eta_1\varepsilon_{31}^*}{\pi}\left[f(a_1,a_2,b_1,b_2) + f(-a_1,-a_2,b_1,b_2)\right] + \frac{\eta_2\varepsilon_{32}^*}{\pi\gamma'}\left[g(a_1,a_2,b_1,b_2) - g(-a_1,-a_2,b_1,b_2)\right], \tag{22}$$

where $\xi = \frac{\mu-\mu'}{\mu+\mu'}$, $\eta_1 = \frac{2\gamma\mu}{\gamma'(\mu+\mu')}$, $\eta_2 = \frac{2\gamma'\mu}{\gamma(\mu+\mu')}$, $\mu = \sqrt{C_{44}C_{55}}$, $\mu' = \sqrt{C'_{44}C'_{55}}$. Here it shall be stressed that when calculating the displacement field in the lower quarter plane, one should use $\frac{\gamma'}{\gamma}x_2$ as a new variable to replace the variable x_2 in Eq. (7), where $\gamma' = \sqrt{C'_{55}/C'_{44}}$.

Equation (21) implies that the induced total displacement in the upper quarter plane of the bimaterial can be considered as the superposition of four rectangular inclusions (region A with eigenstrains ε_{31}^* and ε_{32}^*, image region B with eigenstrains $\xi\varepsilon_{31}^*$ and $-\xi\varepsilon_{32}^*$, image region C with eigenstrains $-\xi\varepsilon_{31}^*$ and $-\xi\varepsilon_{32}^*$, and image region D with eigenstrains $-\varepsilon_{31}^*$ and ε_{32}^*) in an infinite orthotropic plane with elastic properties of the upper quarter plane. On the other hand, Eq. (22) implies that the induced total displacement in the lower quarter plane of the bimaterial can be considered as the superposition of two rectangular inclusions (image region A' (A' : $a_1 \leq x_1 \leq a_2,\ \frac{\gamma}{\gamma'}b_1 \leq x_2 \leq \frac{\gamma}{\gamma'}b_2$) with eigenstrains $\eta_1\varepsilon_{31}^*$ and $\eta_2\varepsilon_{32}^*$, image region D' (D' : $-a_2 \leq x_1 \leq -a_1,\ \frac{\gamma}{\gamma'}b_1 \leq x_2 \leq \frac{\gamma}{\gamma'}b_2$) with eigenstrains $-\eta_1\varepsilon_{31}^*$ and $\eta_2\varepsilon_{32}^*$) in an infinite orthotropic plane with elastic properties of the lower quarter plane.

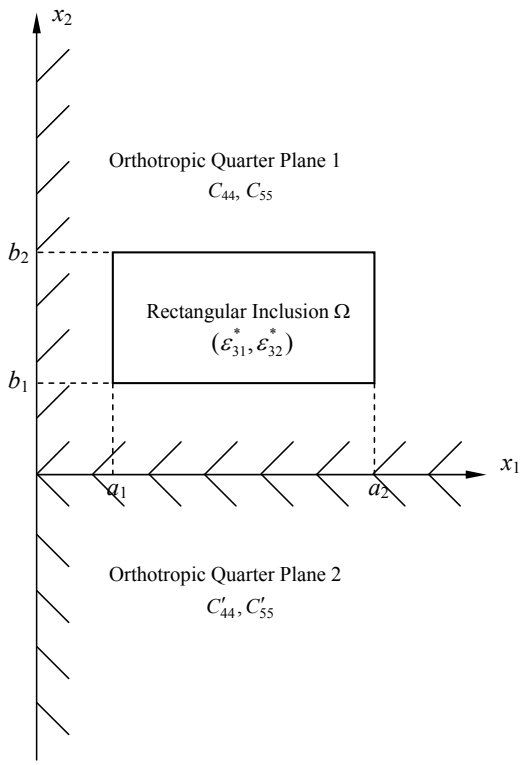

Fig. 2 A rectangular inclusion with uniform antiplane eigenstrains ε^*_{31} and ε^*_{32} embedded in one of the two bonded orthotropic quarter planes.

When the boundary $x_1 = 0$ is fixed, then the total displacement in the upper quarter plane can be expressed as

$$\begin{aligned} u =& \frac{\varepsilon^*_{31}}{\pi}\left[f(a_1,a_2,b_1,b_2) - \xi f(a_1,a_2,-b_1,-b_2) + \xi f(-a_1,-a_2,-b_1,-b_2) - f(-a_1,-a_2,b_1,b_2)\right] \\ &+ \frac{\varepsilon^*_{32}}{\pi\gamma}\left[g(a_1,a_2,b_1,b_2) + \xi g(a_1,a_2,-b_1,-b_2) + \xi g(-a_1,-a_2,-b_1,-b_2) + g(-a_1,-a_2,b_1,b_2)\right], \end{aligned} \tag{23}$$

and the total displacement in the lower quarter plane is

$$u' = \frac{\eta_1\varepsilon^*_{31}}{\pi}\left[f(a_1,a_2,b_1,b_2) - f(-a_1,-a_2,b_1,b_2)\right] + \frac{\eta_2\varepsilon^*_{32}}{\pi\gamma'}\left[g(a_1,a_2,b_1,b_2) + g(-a_1,-a_2,b_1,b_2)\right]. \tag{24}$$

Eq. (23) implies that the induced total displacement in the upper quarter plane of the bimaterial can be considered as the superposition of four rectangular inclusions (region A with eigenstrains ε^*_{31} and ε^*_{32}, image region B with eigenstrains $\xi\varepsilon^*_{31}$ and $-\xi\varepsilon^*_{32}$, image region C with eigenstrains $\xi\varepsilon^*_{31}$ and $\xi\varepsilon^*_{32}$, and image region D with eigenstrains ε^*_{31} and $-\varepsilon^*_{32}$) in an infinite orthotropic plane with elastic properties of the upper quarter plane. On the other hand, Eq. (24) implies that the induced total displacement in the lower quarter plane of the bimaterial can be considered as the superposition of two rectangular inclusions (image region A' with eigenstrains $\eta_1\varepsilon^*_{31}$ and $\eta_2\varepsilon^*_{32}$, image region D' with eigenstrains $\eta_1\varepsilon^*_{31}$ and $-\eta_2\varepsilon^*_{32}$) in an infinite orthotropic plane with elastic properties of the lower quarter plane.

With the induced displacement field, the strains can be obtained by taking the derivative of the displacement with respect to the coordinates, and the stresses by making use of the constitutive relation (1). We also remark that the displacement solutions in the upper quarter plane of the bimaterial can be reduced to those in the quarter plane presented in Sect. 4. More specifically, if the lower quarter plane is much soft compared to the upper quarter plane (i.e., $\mu'/\mu = 0$), we then have $\xi = 1$. Consequently, the bimaterial displacement, Eq. (21), in the upper quarter plane with traction free on $x_1 = 0$, is reduced to the displacement, Eq. (5), for the free-free quarter plane. Similarly, the bimaterial displacement, Eq. (23), in the upper quarter plane with fixed boundary condition on $x_1 = 0$, is reduced to the displacement, Eq. (18), for the fixed-free quarter plane.

5 Numerical examples

We first consider a rectangular inclusion with the dimension $a_2 = 3a_1,\ b_2 = 2b_1 = 2a_1$ in an orthotropic quarter plane with $\gamma = \sqrt{C_{55}/C_{44}} = 1.5$, and we further assume that $\varepsilon^*_{31} \neq 0,\ \varepsilon^*_{32} = 0$. Fig. 3 demonstrates the continuous distribution

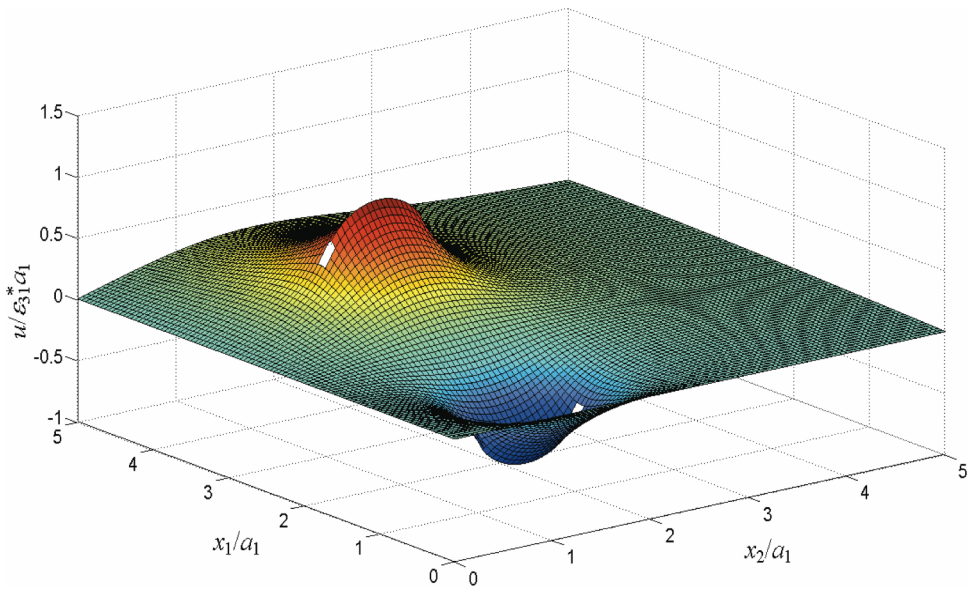

Fig. 3 (online colour at: www.zamm-journal.org) Contour of the normalized displacement for a fixed-fixed quarter plane with $a_2 = 3a_1,\ b_2 = 2b_1 = 2a_1$, and $\gamma = 1.5$ due to the eigenstrain ε_{31}^{*} imposed on the rectangular inclusion.

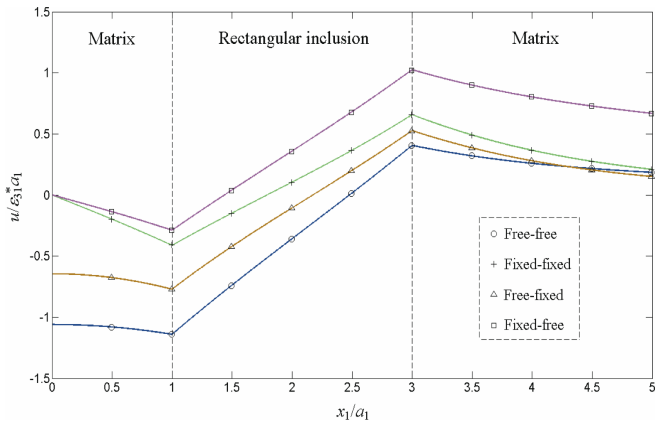

Fig. 4 (online colour at: www.zamm-journal.org) Distribution of the normalized displacement along line segment $0 \le x_1 \le 5a_1$ and $x_2 = b_1$ for the four sets of boundary conditions with $a_2 = 3a_1,\ b_2 = 2b_1 = 2a_1$, and $\gamma = 1.5$ due to the eigenstrain ε_{31}^{*} imposed on the rectangular inclusion.

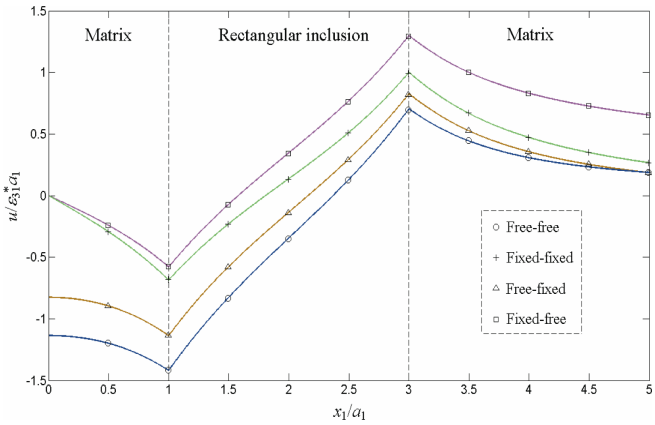

Fig. 5 (online colour at: www.zamm-journal.org) Distribution of the normalized displacement along line segment $0 \le x_1 \le 5a_1$ and $x_2 = (b_1 + b_2)/2$ for the four sets of boundary conditions with $a_2 = 3a_1,\ b_2 = 2b_1 = 2a_1$, and $\gamma = 1.5$ due to the eigenstrain ε_{31}^{*} imposed on the rectangular inclusion.

of the displacement for a fixed-fixed quarter plane. It is apparent that the fixed boundary condition along the two boundaries of the quarter plane is exactly satisfied. The normalized displacement $u/a_1\varepsilon_{31}^{*}$ reaches its maximum value of 1.0003 at the location $x_1 = 3a_1,\ x_2 = 1.53a_1$, and its minimum value of -0.6867 at $x_1 = a_1,\ x_2 = 1.49a_1$. To show more clearly the influence of the boundary conditions on the distribution of the displacement, we present in Figs. 4 to 6 the variations of the displacement along the three parallel line segments $0 \le x_1 \le 5a_1$ and $x_2 = b_1,\ (b_1 + b_2)/2,\ b_2$ for the four sets of boundary conditions discussed in Sect. 3. It is found from Figs. 4 to 6 that the displacement along a certain line segment corresponding to the fixed-free boundary condition is the largest, that to the free-free boundary conditions is the smallest, and those to the fixed-fixed and free-fixed lie in between.

We show in Figs. 7 to 12 the distributions of the two stress components σ_{31} and σ_{32} along the three parallel line segments $0 \le x_1 \le 5a_1$ and $x_2 = b_1,\ (b_1 + b_2)/2,\ b_2$ for the four sets of boundary conditions. Due to the fact that $\varepsilon_{32}^{*} = 0$, the two stress components σ_{31} and σ_{32} are *continuous* along the three line segments. In addition it is observed

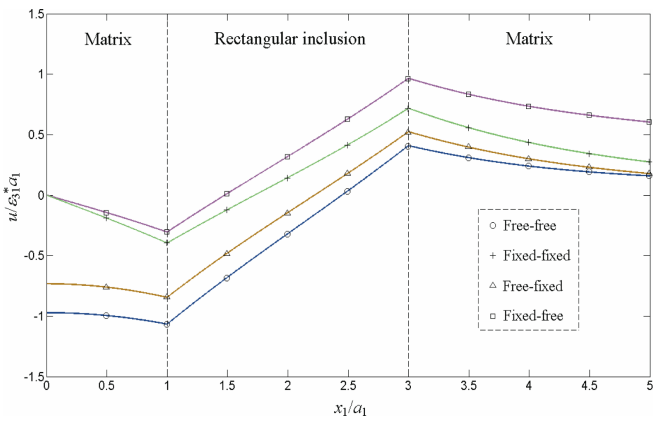

Fig. 6 (online colour at: www.zamm-journal.org) Distribution of the normalized displacement along line segment $0 \leq x_1 \leq 5a_1$ and $x_2 = b_2$ for the four sets of boundary conditions with $a_2 = 3a_1$, $b_2 = 2b_1 = 2a_1$, and $\gamma = 1.5$ due to the eigenstrain ε_{31}^{*} imposed on the rectangular inclusion.

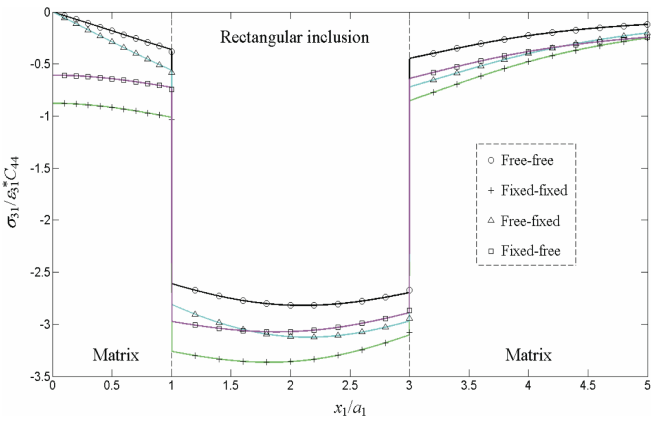

Fig. 7 (online colour at: www.zamm-journal.org) Distribution of the normalized stress component σ_{31} along line segment $0 \leq x_1 \leq 5a_1$ and $x_2 = b_1$ for the four sets of boundary conditions with $a_2 = 3a_1$, $b_2 = 2b_1 = 2a_1$, and $\gamma = 1.5$ due to the eigenstrain ε_{31}^{*} imposed on the rectangular inclusion.

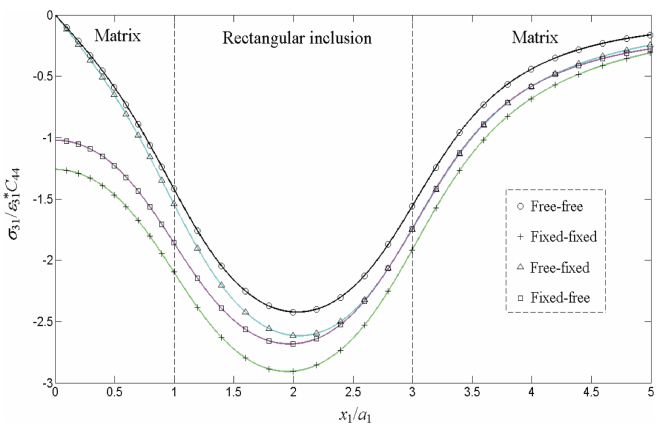

Fig. 8 (online colour at: www.zamm-journal.org) Distribution of the normalized stress component σ_{31} along line segment $0 \leq x_1 \leq 5a_1$ and $x_2 = (b_1 + b_2)/2$ for the four sets of boundary conditions with $a_2 = 3a_1$, $b_2 = 2b_1 = 2a_1$, and $\gamma = 1.5$ due to the eigenstrain ε_{31}^{*} imposed on the rectangular inclusion.

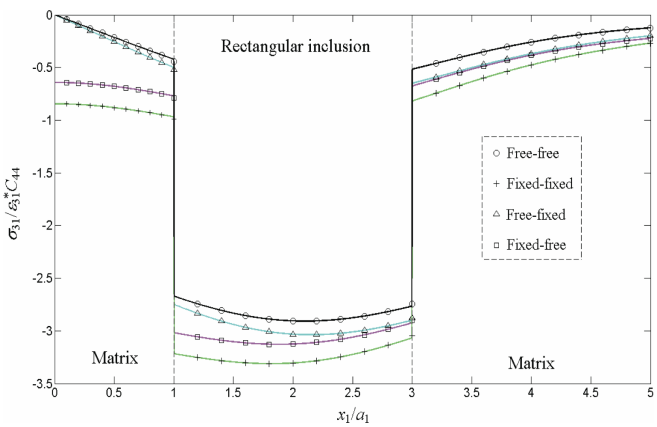

Fig. 9 (online colour at: www.zamm-journal.org) Distribution of the normalized stress component σ_{31} along line segment $0 \leq x_1 \leq 5a_1$ and $x_2 = b_2$ for the four sets of boundary conditions with $a_2 = 3a_1$, $b_2 = 2b_1 = 2a_1$, and $\gamma = 1.5$ due to the eigenstrain ε_{31}^{*} imposed on the rectangular inclusion.

from Figs. 7 and 9 that the value of the stress component σ_{31} undergoes a significant change when crossing the corners of the rectangular inclusion. It is further observed from Figs. 10 and 12 that the stress component σ_{32} is singular at the corners of the rectangular inclusion, which is in agreement with our previous theoretical analysis in Sect. 3. The requirements that $\sigma_{31} = 0$ at $x_1 = 0$ for the free-free and free-fixed boundary conditions and $\sigma_{32} = 0$ at $x_1 = 0$ for the fixed-fixed and fixed-free boundary conditions are clearly satisfied in Figs. 7 to 12. It is well known that either the non-elliptical shape of the inclusion or the existence of a nearby boundary can induce non-uniform stress distributions inside the inclusion [11]. Consequently the observed non-uniform stresses in Figs. 7 to 12 inside the rectangular inclusion in a quarter plane are due to the non-elliptical shape of the rectangular inclusion as well as the existence of the neighboring two boundaries $x_1 = 0$ and $x_2 = 0$. The normalized stress component $\sigma_{31}/C_{44}\varepsilon_{31}^{*}$ along a certain line segment in Figs. 7 to 9 reaches its minimum value at the location very close to $x_1 = (a_1 + a_2)/2$. The magnitude of σ_{32} induced by the eigenstrain ε_{31}^{*} is rather small as compared to that of σ_{31} when the observation point is away from the corners (see Figs. 8 and 11).

Figures 13 to 15 illustrate the distribution of stress component σ_{31} along the three parallel line segments $0 \leq x_2 \leq 3a_1$ and $x_1 = a_1$, $(a_1 + a_2)/2$, a_2 for the four sets of boundary conditions. It is observed from Figs. 13 to 15 that σ_{31} is discontinuous across the interfaces $x_2 = b_1(= a_1)$ and $x_2 = b_2(= 2a_1)$, and the discontinuity is exactly $\left(\sigma_{31}^{\text{inclusion}} - \sigma_{31}^{\text{matrix}}\right)/\varepsilon_{31}^{*}C_{44} = -2\gamma^2 = -4.5$, as predicted in Sect. 3. In addition the maximum magnitude of σ_{31} along

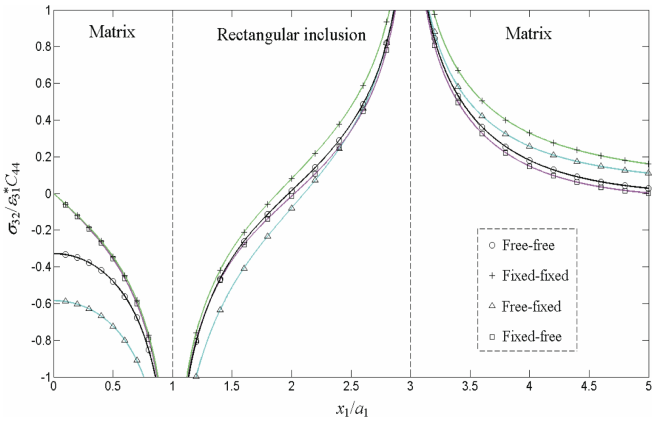

Fig. 10 (online colour at: www.zamm-journal.org) Distribution of the normalized stress component σ_{32} along line segment $0 \le x_1 \le 5a_1$ and $x_2 = b_1$ for the four sets of boundary conditions with $a_2 = 3a_1$, $b_2 = 2b_1 = 2a_1$ and $\gamma = 1.5$ due to the eigenstrain ε_{31}^* imposed on the rectangular inclusion.

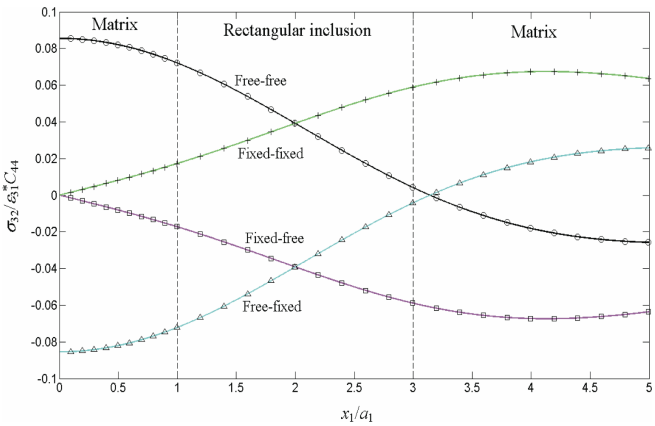

Fig. 11 (online colour at: www.zamm-journal.org) Distribution of the normalized stress component σ_{32} along line segment $0 \le x_1 \le 5a_1$ and $x_2 = (b_1 + b_2)/2$ for the four sets of boundary conditions with $a_2 = 3a_1$, $b_2 = 2b_1 = 2a_1$, and $\gamma = 1.5$ due to the eigenstrain ε_{31}^* imposed on the rectangular inclusion.

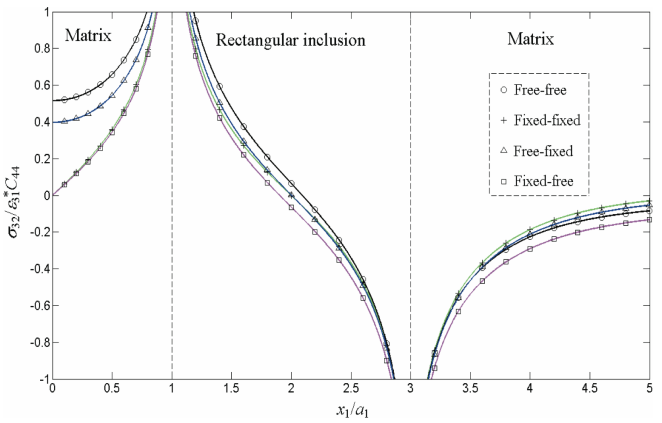

Fig. 12 (online colour at: www.zamm-journal.org) Distribution of the normalized stress component σ_{32} along line segment $0 \le x_1 \le 5a_1$ and $x_2 = b_2$ for the four sets of boundary conditions with $a_2 = 3a_1$, $b_2 = 2b_1 = 2a_1$, and $\gamma = 1.5$ due to the eigenstrain ε_{31}^* imposed on the rectangular inclusion.

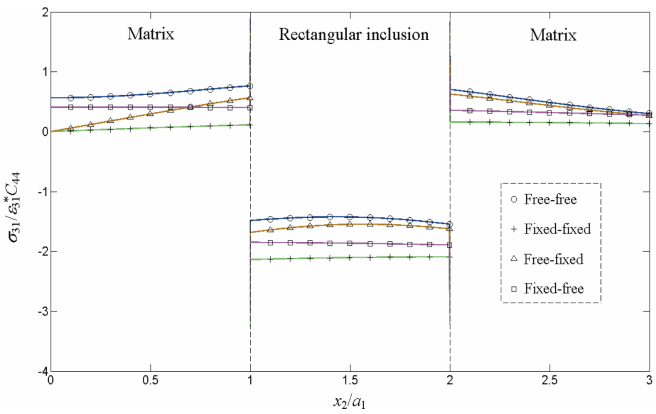

Fig. 13 (online colour at: www.zamm-journal.org) Distribution of the normalized stress component σ_{31} along line segment $0 \le x_2 \le 3a_1$ and $x_1 = a_1$ for the four sets of boundary conditions with $a_2 = 3a_1$, $b_2 = 2b_1 = 2a_1$, and $\gamma = 1.5$ due to the eigenstrain ε_{31}^* imposed on the rectangular inclusion.

a certain line segment always occurs at the inclusion side of the interface $x_2 = b_1$ where the horizontal surface $x_2 = 0$ is fixed and at the inclusion side of the interface $x_2 = b_2$ where the horizontal surface $x_2 = 0$ is traction free. Due to the existence of the horizontal surface $x_2 = 0$, the distribution of σ_{31} is not symmetric with respect to $x_2 = (b_1 + b_2)/2$.

As for the bimaterial case, we consider the upper S-Glass Epoxy quarter plane bonded to the lower AS4/8552 quarter plane. S-Glass Epoxy and AS4/8552 have been widely adopted in commercial aircraft structures. The material constants of S-Glass Epoxy are $C_{44} = 4.8$ GPa and $C_{55} = 5.5$ GPa, and those of AS4/8552 are $C_{44} = 10.5628$ GPa and $C_{55} = 7.17055$ GPa [12]. Consequently, $\gamma = 1.0704$, $\gamma' = 0.8239$, $\xi = -0.2576$ and $\eta = 1.2576$. Shown in Fig. 16 is the distribution of the stress component σ_{32} (or traction) along the positive x_1-axis ($x_2 = 0$) when the location of the inclusion varies vertically with different b_1 ($a_2 = 3a_1$, $b_2 = b_1 + a_1$), due to the eigenstrain ε_{31}^* imposed on the rectangular inclusion. Traction free condition is assumed along the boundary line $x_1 = 0$. It is observed that the interfacial traction exhibits singular behavior at points $x_1 = a_1$ and $x_1 = 3a_1$ when the lower edge of the rectangular inclusion lies on the x_1-axis, i.e., $b_1 = 0$ (the two points $x_1 = a_1$ and $x_1 = 3a_1$ then become also two of the corners of the rectangle). As a result interface damage could be induced due to the stress concentration. As the inclusion moves further away from the interface, on the other hand, the magnitude of the traction on the interface decreases. The inclusion with $b_1 = 5a_1$ induces the minimal interface traction along the line.

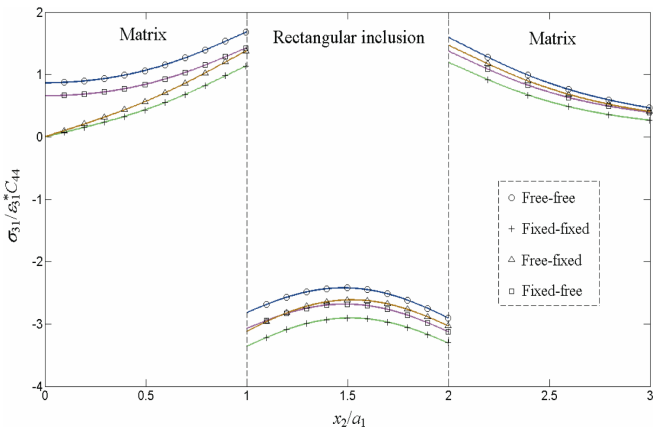

Fig. 14 (online colour at: www.zamm-journal.org) Distribution of the normalized stress component σ_{31} along line segment $0 \leq x_2 \leq 3a_1$ and $x_1 = (a_1 + a_2)/2$ for the four sets of boundary conditions with $a_2 = 3a_1,\ b_2 = 2b_1 = 2a_1$, and $\gamma = 1.5$ due to the eigenstrain ε_{31}^{*} imposed on the rectangular inclusion.

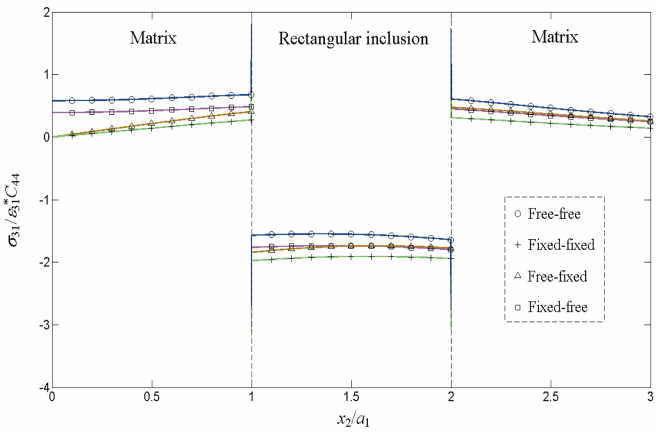

Fig. 15 (online colour at: www.zamm-journal.org) Distribution of the normalized stress component σ_{31} along line segment $0 \leq x_2 \leq 3a_1$ and $x_1 = a_2$ for the four sets of boundary conditions with $a_2 = 3a_1,\ b_2 = 2b_1 = 2a_1$, and $\gamma = 1.5$ due to the eigenstrain ε_{31}^{*} imposed on the rectangular inclusion.

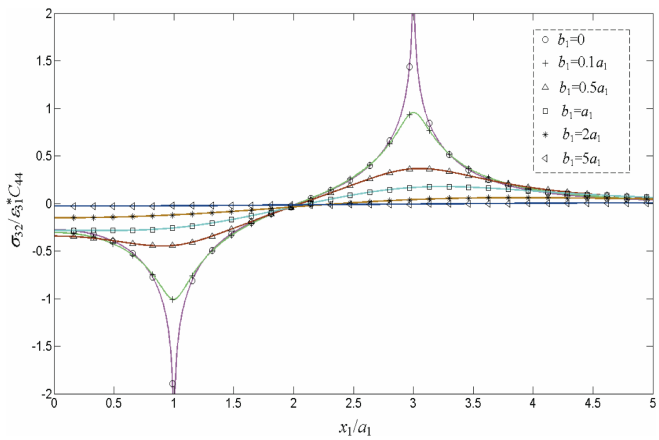

Fig. 16 (online colour at: www.zamm-journal.org) Distribution of the normalized traction σ_{32} along positive x_1-axis ($x_2 = 0$) when the location of the inclusion changes vertically with b_1 ($a_2 = 3a_1,\ b_2 = b_1 + a_1$) due to the eigenstrain ε_{31}^{*} imposed on the rectangular inclusion embedded in orthotropic bimaterial. Traction free condition is assumed along the boundary line $x_1 = 0$.

6 Concluding remarks

By employing the explicit expressions of Green's functions for an orthotropic quarter plane and a bimaterial composed of two bonded orthotropic quarter planes recently derived by Ting [10], we derived exact closed-form solutions in terms of elementary functions for the displacement, strains, and stresses induced by a rectangular inclusion embedded in an orthotropic quarter plane or in one of the two bonded orthotropic quarter planes. Numerical examples are presented to validate the solutions and to demonstrate the influence of the boundary conditions on the induced displacements and stresses. An extension of the present results to the in-plane deformation seems difficult due to the fact that the expressions of the Green's functions for a bimaterial composed of two isotropic quarter planes are too complicated to be used in the analysis of the corresponding inclusion problem [13].

Acknowledgements The authors are greatly indebted to the reviewers for their very helpful comments and suggestions. This work is partially supported by AFOSR/AFRL and ARO/ARL.

References

[1] Y. P. Chiu, On the stress field due to initial strains in a cuboid surrounded by an infinite elastic space, ASME J. Appl. Mech. **44**, 587–590 (1977).
[2] T. Mura, Micromechanics of Defects in Solids (Martinus Nijhoff, Hague, The Netherlands 1982).
[3] H. Nozaki and M. Taya, Elastic fields in polygonal-shaped inclusion with uniform eigenstrains, ASME J. Appl. Mech. **64**, 495–502 (1997).

[4] E. Pan and X. Jiang, Singularity analysis at the vertex of polygonal quantum wire inclusions, Mech. Res. Commun. **33**, 1–8 (2001).
[5] Y. P. Chiu, On the stress field and surface deformation in a half space with a cuboidal zone in which initial strains are uniform, ASME J. Appl. Mech. **45**, 302–306 (1978).
[6] C. M. Hu, Stress from a parallelepipedic thermal inclusion in a semispace, J. Appl. Phys. **66**, 2741–2743 (1989).
[7] F. Glas, Coherent stress relaxation in a half space: modulated layers, inclusions, steps, and a general solution, J. Appl. Phys. **70**, 3556–3571 (1991).
[8] E. Pan, Eshelby problem of polygonal inclusions in anisotropic piezoelectric full- and half-planes, J. Mech. Phys. Solids **52**, 567–589 (2004).
[9] E. Pan, Eshelby problem of polygonal inclusions in anisotropic piezoelectric bimaterials, Proc. R. Soc. Lond. **A460**, 537–560 (2004).
[10] T. C. T. Ting, Green's functions for a bimaterial consisting of two orthotropic quarter planes subjected to an antiplane force and a screw dislocation, Math. & Mech. Solids. **10**, 197–211 (2005).
[11] C. Q. Ru, Analytic solution for Eshelby's problem of an inclusion of arbitrary shape in a plane or half-plane, ASME J. Appl. Mech. **66**, 315–322 (1999).
[12] N. Tullini, M. Savoia, and C. O. Horgan, End effects for antiplane shear deformations of periodically laminated strips with imperfect bonding, J. Elast. **50**, 227–244 (1998).
[13] P. A. Martin, On Green's function for a bimaterial elastic half-plane, Int. J. Solids & Struct. **40**, 2101–2119 (2003).

Book Reviews

W. Hauger, V. Mannl, W. Wall und E. Werner, Aufgaben zu Technische Mechanik 1–3. Statik, Elastostatik, Kinetik, 6., korr. Auflage Springer-Verlag Berlin 2008, 420 S, Softcover, ISBN: 978-3-540-77691-8

Das studienbegleitende Übungsbuch soll zum eigenständigen Lösen von Aufgaben des Grundkurses Technische Mechanik beitragen. Bei einer 6. Auflage kann man davon ausgehen, dass sich das Konzept der Autoren bewährt hat. Im Mittelpunkt stehen eine kurze Formelsammlung (diese ersetzt nicht die Vorlesung!), den entsprechenden Kapiteln des Grundkurses zugeordnete Aufgaben sowie ausführliche durchgerechnete Lösungen.

Für die nächste Auflage sollte überlegt werden, ob einige Elemente aus dem bisherigen Konzept weggelassen werden können. Hierzu gehören insbesondere die Mohrschen Spannungskreise, die heute in der Praxis eine geringere Rolle spielen. Gleiches gilt für die Tafel der Integrale. Eine weitere Anregung betrifft das Layout. In den zugehörigen Lehrbüchern wurde in den letzten Auflagen auch mehrfarbig gedruckt. Dies sollte hier auch geschehen, da es das Lesen und Verstehen erleichtert.

Halle (Saale) **Holm Altenbach**

J. N. Reddy, Theory and Analysis of Elastic Plates and Shells, 2nd ed., CRC Press, Taylor & Francis Group, Boca Raton, FL, 2007, 568 pp., £ 49.99,
ISBN: 978-0-8493-8415-8

This is a revised and updated version of the well-known textbook published by J.N. Reddy several years ago. It includes basics of the plate theory, variational methods, energy principles, classical and Finite Element based solution techniques. It can be recommended as a textbook on this topic in aerospace, civil, and mechanical engineering.

The weakest point of this book is that the author is focused mostly on his own research. During the last years there have been many new contributions to this topic, which are not reflected enough. The reader expects as a minimum some information about new trends, alternative approaches, etc. In addition, it seems that the chapter about the shear deformation plate theories is incomplete. At first, there are other, quite different contributions (e.g. Reissner's theory) and the criticism to the first order theories should be added by the criticism to the third order theory.

Halle (Saale) **Holm Altenbach**

